Rafał Grzejda

Assistant Professor
West Pomeranian University of Technology
Faculty of Mechanical Engineering and
Mechatronics
in Szczecin
Poland

Arkadiusz Parus

Head of the Environmental Measurement
Laboratory
West Pomeranian University of Technology
Faculty of Mechanical Engineering and
Mechatronics
in Szczecin
Poland

Health Assessment of a Multi-Bolted Connection due to Removing Selected Bolts

In the paper, experimental studies of an asymmetric preloaded seven-bolted connection are presented. The tightening process of the connection was carried out with a wrench, monitoring the values of the bolt forces with a calibrated strain gauge measuring system. Two methods of bolt tightening were tested: in one and several passes. After all bolts were tightened, the selected bolts were removed, simulating bolt failure under the loading conditions of the connection. The influence of the method and sequence of bolt tightening on the distribution of bolt forces values after the introduction of failure states of some bolts was investigated. The results were statistically processed and presented in the form of graphs showing the distributions of normalised bolt forces values for all the considered failure cases.

Keywords: bolt tightening sequence, multi-bolted connection assembly, preload monitoring, resistance strain gauges.

1. INTRODUCTION

Bolted and multi-bolted connections are among the most commonly used temporary fastenings in both mechanical and structural engineering [1-3]. Various experimental studies on these connections are still undertaken by many authors.

Recently, a lot of attention has been paid to research in the field of structural health monitoring of bolts and bolted connections under the influence of the loss of load capacity of the supporting element of the structure. Kozłowski and Kukla [4], and Kukla and Kozlowski [5] described experimental tests of unstiffened two-sided connections with a flush and extended end plate, which consisted in checking the behaviour of the structure due to the loss of one of the columns. Similar tests were performed by Xu *et al*. [6], and Gao *et al*. [7]. Expe–rimental investigation of steel moment frames subjected to column loss were carried out by Marginean *et al*. [8]. In contrast, the progressive collapse mechanism of bolted structures were analysed, among others, by Tang *et al*. [9], Wang *et al*. [10], and Chen *et al*. [11].

On the other hand, less attention has been paid to experimental research in the field of structural health monitoring of bolts and bolted connections due to loss of load capacity of selected fasteners in the connection. Li and Hao [12] monitored the state of bolted connections in a truss bridge model due removing selected bolts. Yan *et al*. [13] described an experimental validation of a damage detection method on a full-scale highway sign support truss. As one of the simulated failures, they considered the loss of all bolts in one of the flange connection in this truss. Pham and Hancock [14], and Pham *et al*. [15] investigated deformations of

connections of beams with cold-formed C-sections for different number of bolt rows. There are also only a few papers on modelling the phenomena occurring in bolted connections under the influence of fasteners failure [16-19]. Therefore, this subject has been taken up in the presented paper.

An indispensable part of assessing the structural condition of bolted connections is monitoring of bolt forces and detection of joint loosening. They are implemented in many ways. The change in magnetic flux density as a diagnostic parameter of the bolt tightening torque was used by Mori *et al*. [20]. The papers by Yasui *et al*. [21], Kim and Hong [22], Blachowski *et al*. [23], and Pan *et al*. [24] were written on the subject of ultrasonic measurement of axial stress in bolts. Monitoring of bolt forces can also be carried out using embedded fiber Bragg gratings (FBG) sensors [25]-[28]. Martinez *et al*. [29], Zhang *et al*. [30], and Wang *et al*. [31] applied acoustic methods to monitor bolt loosening, while for the same purpose Wang *et al*. [32], Wang *et al*. [33], Huynh *et al*. [34], and Na [35] used impedance methods. Nazarko and Ziemianski [36] applied the phenomenon of elastic wave propagation, introduced and measured by piezoelectric transducers, to identify the forces in the bolts in a flange connection. The relationships between the measured signal changes and the variations of the forces in the bolts were assessed in this case using artificial neural networks. Sun *et al*. [37] proposed a bolt-loosening detection method based on the binocular vision. In addition, vision-based methods for the bolts looseness detection were also presented by Wang *et al*. [38], and Huynh [39]. Sidorov *et al*. [40] designed and implemented sensor nodes (named TenSense M20) for continuous remote structural health monitoring of bolted connections.

However, the most common method of measuring bolt forces is the method based on the use of resistance strain gauges. The measurements are made by means of strain gauges glued to the outside of the bolt shank [41]-

[46], inserted into the hole inside the bolt shank [47-51] or on the bolt head [52]. In addition to ultrasonic sensing, it is the method with the highest accuracy [36]. Therefore, this method has been also implemented in the presented paper.

Experimental tests of the process of tightening multi-bolted connections are carried out mainly for connections showing geometric symmetry or load symmetry. These studies include tightening in one pass [53-55] and in several passes [56-58]. In this study, these two types of tightening were also used. However, in order to make the research universal, it was performed for the case of asymmetric multi-bolted connection. The research is an extension of the paper [45] and will be used to validate the modelling method of the tightening process of arbitrary multi-bolted connections presented in [59,60].

The paper is structured as follows: Section 2 des– cribes the research stand and research procedure, including details of tightening methods and scenarios of simulated failure of the tested multi-bolted connection. Section 3 focuses on results of the research as well as a discussion about them. Section 4 gives some additional conclusions from the conducted research.

2. RESEARCH STAND AND PROCEDURE

The geometry of the tested connection and the assumptions made at the design stage are described in detail in [45]. Only general information on this subject will be presented in this paper. The diagram of the multi-bolted connection is shown in Fig. 1a.
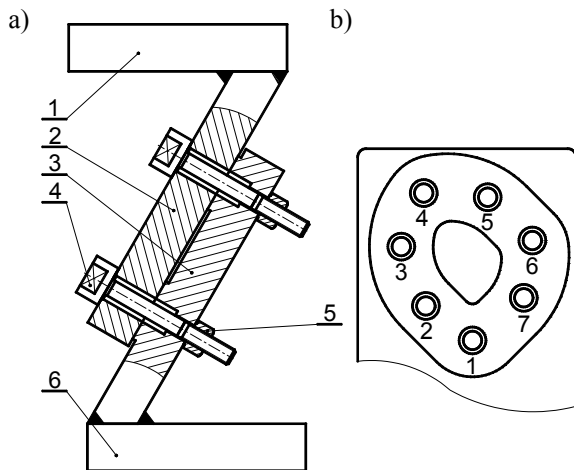

Figure 1. Diagram of the tested multi-bolted connection (a) and view of the contact surface between the joined elements (b) (1 – upper plate; 2, 3 – joined elements; 4 – M10x1.25 bolt; 5 – high hexagonal nut; 6 – base)

It consists of two joined elements (2) and (3), fastened with seven M10x1.25 bolts (4) and nuts (5). The element (2) is welded to the upper plate (1), and the element (3) to the base (6). The connection is tilted relative to the base (6) by 60 deg. All the joined elements are made of 1.0577 steel. The bolts are made in the mechanical property class 8.8, and the nuts in the mechanical property class 8.

The contact surface between the joined elements and the adopted bolt numbering are shown in Fig. 1b.

The force changes in each bolt were measured using four TENMEX TFxy-4/120 strain gauges with two axes of measuring ladders arranged perpendicularly to each other. The strain gauges were glued to the bolt shanks in a full strain gauge bridge configuration (Fig. 2). The view of the bolts prepared for the measurements is shown in Fig. 3.
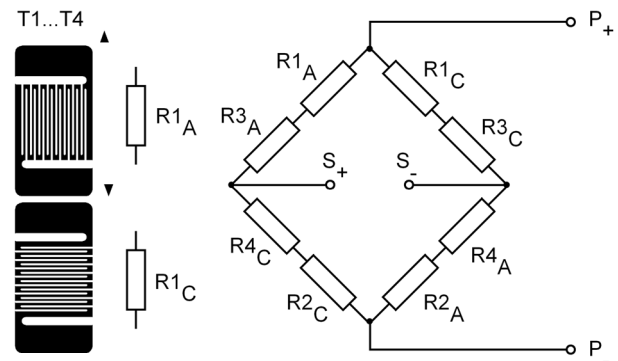

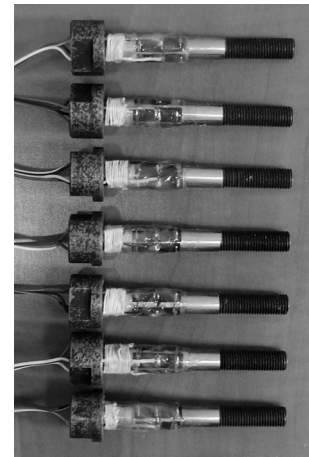**Figure 2. Diagram of the strain gauge system glued to a single bolt**

Figure 3. View of the bolts

Before the beginning of the study, each of the bolts was calibrated on the Instron 8850 testing machine [46]. As a result of this calibration, a set of regression equations was obtained for the bolts loading and unloading processes in the form:

$$F_{ci} = a_i \cdot V_i \qquad (1)$$

where F_{ci} denotes the calibration axial force of the i-th bolt, a_i is the slope of the regression curve, and V_i denotes the voltage (for $i = 1, 2, …, 7$).
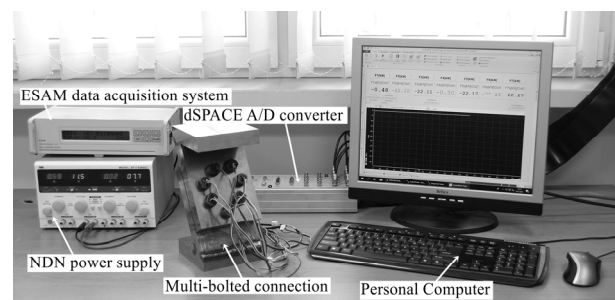

Figure 4. View of the research stand

The above equations were used to determine the forces in the bolts based on the voltmeter indications

and through the program written in the MATLAB R2018b Simulink (Fig. 4).

Table 1. Methods of the multi-bolted connection assembly

Symbol	Description	Value
Tightening in one pass		
F_{pi}	preload of the *i*-th bolt	$F_{pi} = 22$ kN
Tightening in three passes		
F_{pi1}	preload of the *i*-th bolt in the first pass	$0.2 \cdot F_{pi} = 4.4$ kN
F_{pi2}	preload of the *i*-th bolt in the second pass	$0.6 \cdot F_{pi} = 13.2$ kN
F_{pi3}	preload of the *i*-th bolt in the third pass	$F_{pi} = 22$ kN

Table 2. Sequences of tightening the multi-bolted connection

Path type	Sequence
1	1-2-3-4-5-6-7
2	1-3-5-7-2-4-6
3	1-4-7-3-6-2-5
4	1-5-2-6-3-7-4
5	1-6-4-2-7-5-3
6	1-7-6-5-4-3-2

Table 3. States of the connection failure simulation

State	Scheme
After preload	
State 1	
State 2	

The value of the bolts preload F_p was determined as equal to 22 kN based on the PN-EN 1993-1-8 standard [61] and the analysis of the permissible surface pressure values between the nuts and the lower joined element.

The bolts were tightened with a wrench and the force values in the bolts were controlled by the measuring system shown in Fig. 4. The process of tightening the multi-bolted connection was carried out for two assembly methods: in one pass (the bolts were tightened immediately to the full preload value F_p) and in three passes (in the first pass, the bolts were preloaded to the value of $0.2 \cdot F_p$, while in the second and third pass to the value of $0.6 \cdot F_p$, and F_p, respectively).

A summary of information on the assembly methods is shown in Table 1. In both assembly methods, the bolts were tightened sequentially according to the paths shown in Table 2.

After tightening all the bolts, the connection failure was simulated by removing selected bolts. Two states of this analysis were introduced, shown in Table 3.

Each experiment was repeated three times. The further part of the paper presents the values of bolt forces understood as the arithmetic mean of the data obtained in these experiments.

3. RESEARCH RESULTS

The distributions of the mean values of forces F_{pi} in the bolts in relation to the value of the initial force F_{p0} in the case of failure states of the bolts after tightening the multi-bolted connection in one pass are presented in Fig. 5. Figure 6 shows similar diagrams for the case of tightening the connection in three passes.

Based on the analysis of the graphs in Figs. 5 and 6, the following conclusions can be drawn:
1. At the connection failure state, the greatest increases in force occur in bolts in the immediate vicinity of the bolt removed at a given state.
2. The variability of the bolt force values in the connection failure state depends on the sequence of bolt tightening.

The comparative analysis of the waveforms presented in Figs. 5 and 6 was carried out on the basis of the Z_1 index defined as:

$$Z_1 = \left| \frac{F_{pi}^{ap} - F_{pi}^{S}}{F_{pi}^{ap}} \right| \cdot 100 \qquad (2)$$

where F_{pi}^{ap} denotes the force in *i*-th bolt in the considered distribution of forces after the tightening process, and F_{pi}^{S} denotes the force in *i*-th bolt at the given connection failure state.

The maximum values of the Z_1 index obtained for individual tightening methods and the connection failure states are presented in Table 4. Based on its analysis, it can be concluded that the maximum force increments in the bolts caused by the assumed failure states do not depend on the method and sequence of bolt tightening. They are generally in the range of 0.51 to 0.76%.
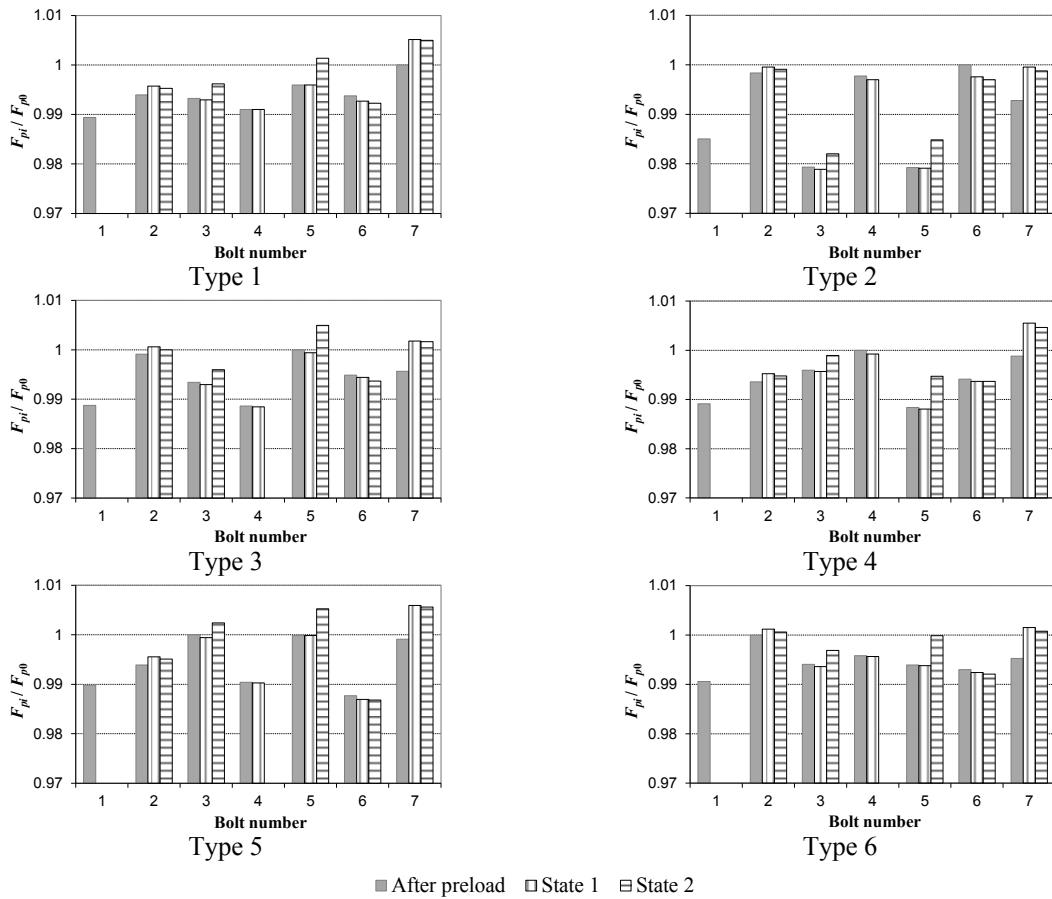
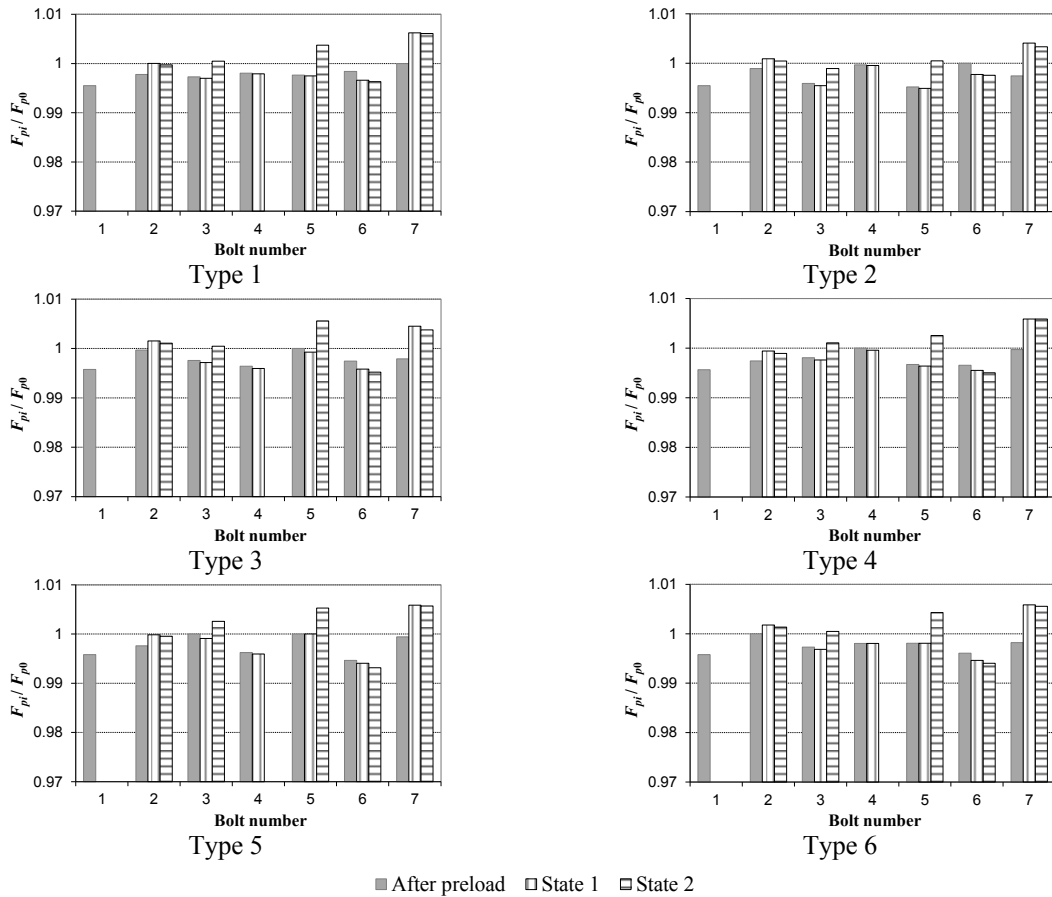Figure 5. Distributions of the bolt forces in the case of tightening the connection in one pass

Figure 6. Distributions of the bolt forces in the case of tightening the connection in three passes
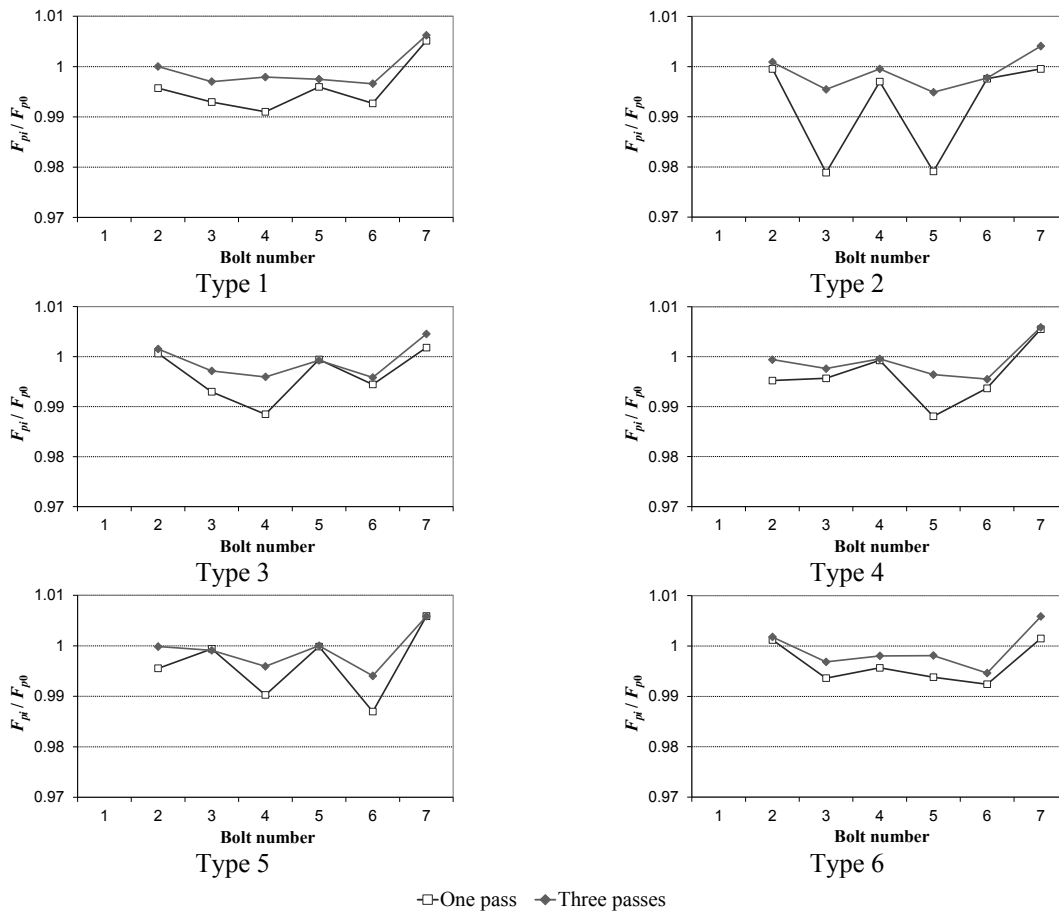
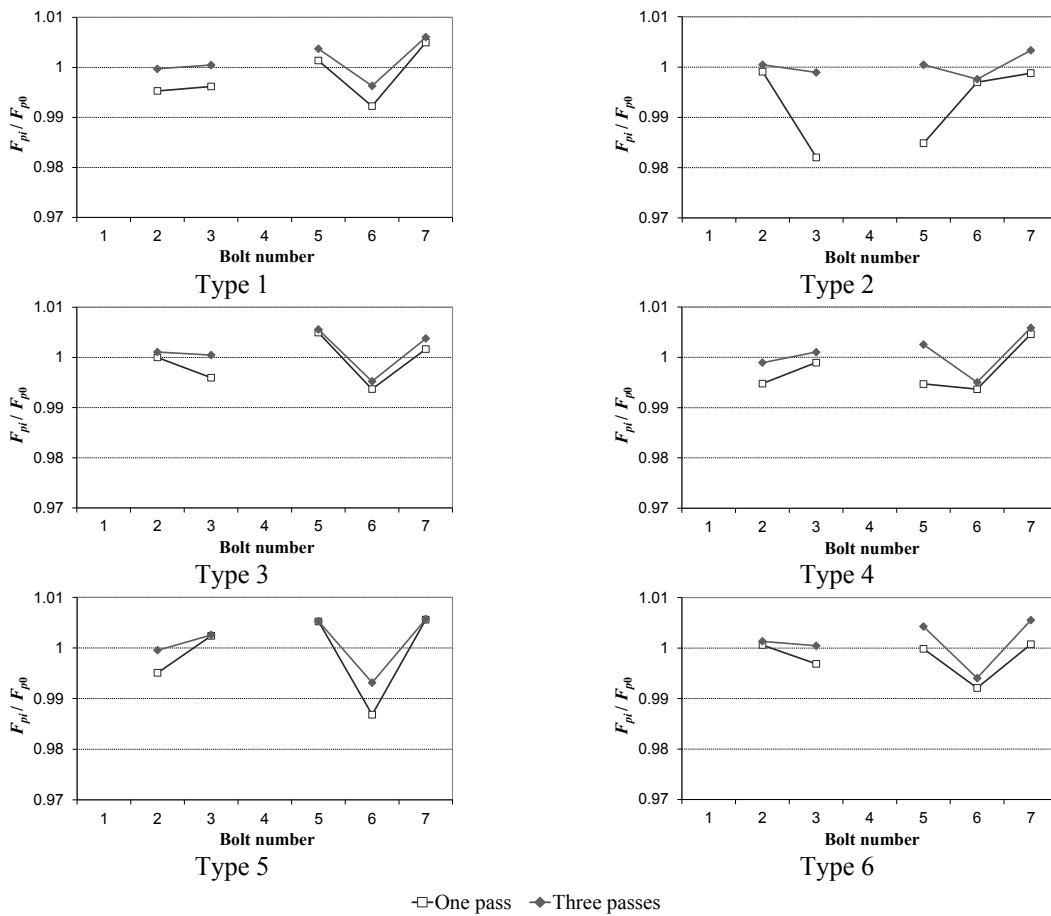Figure 7. Distributions of the bolt forces in the State 1

Figure 8. Distributions of the bolt forces in the State 2

Table 4. Z_1 index values (%)

Path type	Tightening in one pass		Tightening in three passes	
	State 1	State 2	State 1	State 2
1	0.51	0.54	0.62	0.61
2	0.68	0.57	0.67	0.53
3	0.62	0.50	0.66	0.56
4	0.67	0.64	0.62	0.59
5	0.68	0.54	0.65	0.53
6	0.63	0.60	0.76	0.62

The distributions of the mean values of forces F_{pi} in the bolts in relation to the value of the initial force F_{p0} at the end of State 1 of the multi-bolted connection failure, depending on the method of performing the tightening process are presented in Fig. 7. Figure 8 shows similar diagrams for the case of State 2 of the multi-bolted connection failure.

Based on the analysis of the graphs in Figs. 7 and 8, the following conclusions can be drawn:
1. The distributions of the preload in individual bolts in the connection failure state are characterised by some unevenness.
2. The variability of the bolt force value in the connection failure state is smaller in the case of tightening the multi-bolted connection in three passes than in the case of tightening in one pass.

The comparative analysis of the waveforms presented in Figs. 7 and 8 was carried out on the basis of the Z_2 index defined as:

$$Z_2 = \left| \frac{F_{pi}^{onep} - F_{pi}^{threep}}{F_{pi}^{onep}} \right| \cdot 100 \qquad (3)$$

where F_{pi}^{onep} denotes the force in i-th bolt in the considered distribution of forces after the tightening process in one pass, and F_{pi}^{threep} denotes the force in i-th bolt in the considered distribution of forces after the tightening process in three passes.

The maximum values of the Z_2 index obtained for individual tightening methods and the connection failure states are presented in Table 5. Based on its analysis, it can be concluded that the maximum differences in the values of bolt forces achieved for the compared tightening methods slightly depend on the sequence of bolt tightening. They are generally in the range of 0.43 to 1.72%.

Table 5. Z_2 index values (%)

Path type	State 1	State 2
1	0.70	0.44
2	1.69	1.72
3	0.76	0.45
4	0.84	0.79
5	0.72	0.64
6	0.43	0.48

4. CONCLUDING REMARKS

The paper presents an original laboratory stand intended for testing a selected asymmetric multi-bolted con–nection under the conditions of initial tightening the connection. The influence of the method and sequence of bolt tightening on the distribution of force values in bolts after the introduction of selected states of bolts failure was demonstrated. The stand can be used for further studies in the field of assessing the influence of removing selected bolts in the connection subjected to external loads on a testing machine.

REFERENCES

[1] Kędra, R. and Rucka, M.: Preload monitoring in a bolted joint using Lamb wave energy, B. Pol. Acad. Sci. - Tech., Vol. 67, No. 6, pp. 1161-1169, 2019.

[2] Novoselac, S., Kozak, D., Ergić, T. and Damjanović, D.: Fatigue of shaft flange bolted joints under preload force and dynamic response, FME Trans., Vol. 42, No. 4, pp. 269-276, 2014.

[3] Jaszak, P.: Prediction of the durability of a gasket operating in a bolted-flange-joint subjected to cyclic bending, Eng. Fail. Anal., Vol. 120, Paper No. 105027, 2021.

[4] Kozłowski, A. and Kukla, D.: Experimental tests of steel unstiffened double side joints with flush and extended end plate, Archives of Civil Eng., Vol. 65, No. 4, pp. 127-154, 2019.

[5] Kukla, D. and Kozlowski, A.: Parametric study of steel flush and extended end-plate joints under column loss scenario, Eng. Struct., Vol. 237, Paper No. 112204, 2021.

[6] Xu, M., Gao, S., Zhang, S. and Li, H.: Experimental study on bolted CFST-column joints with different configurations in accommodating column-loss, J. Constr. Steel Res., Vol. 151, pp. 122-131, 2018.

[7] Gao, S., Xu, M., Fu, F. and Guo, L.: Performance of bolted steel-beam to CFST-column joints using stiffened angles in column-removal scenario, J. Constr. Steel Res., Vol. 159, pp. 459-475, 2019.

[8] Marginean, I., Dinu, F. and Dubina, D.: Simulation of the dynamic response of steel moment frames following sudden column loss. Experimental calibration of the numerical model and application, Steel Constr., Vol. 11, No. 1, pp. 57-64, 2018.

[9] Tang, H., Deng, X., Jia, Y., Xiong, J. and Peng, C.: Study on the progressive collapse behavior of fully bolted RCS beam-to-column connections, Eng. Struct., Vol. 199, Paper No. 109618, 2019.

[10] Wang, J.-X., Yang, Y., Xian, W. and Li, Q.-Y.: Progressive collapse mechanism analysis of concrete-filled square steel tubular column to steel beam joint with bolted-welded hybrid connection, Int. J. Steel Struct., Vol. 20, No. 5, pp. 1618-1635, 2020.

[11] Chen, C., Qiao, H., Wang, J. and Chen, Y.: Progressive collapse behavior of joints in steel moment frames involving reduced beam section, Eng. Struct., Vol. 225, Paper No. 111297, 2020.

[12] Li, J. and Hao, H.: Health monitoring of joint conditions in steel truss bridges with relative displacement sensors, Measurement, Vol. 88, pp. 360-371, 2016.

[13] Yan, G., Dyke, S.J. and Irfanoglu, A.: Experimental validation of a damage detection approach on a full-scale highway sign support truss, Mech. Syst. Signal Pr., Vol. 28, pp. 195-211, 2012.

[14] Pham, C.H. and Hancock, G.J.: Tension field action for cold-formed sections in shear, J. Constr. Steel Res., Vol. 72, pp. 168-178, 2012.

[15] Pham, C.H, Zelenkin, D. and Hancock, G.J.: Effect of flange restraints on shear tension field action in cold-formed C-sections, J. Constr. Steel Res., Vol. 129, pp. 42-53, 2017.

[16] Rucka, M., Zima, B. and Kędra, R.: Application of guided wave propagation in diagnostics of steel bridge components, Archives of Civil Eng., Vol. 60, No. 4, pp. 493-515, 2014.

[17] Qin, Z., Han, Q. and Chu, F.: Bolt loosening at rotating joint interface and its influence on rotor dynamics, Eng. Fail. Anal., Vol. 59, 456-466. 2016.

[18] Blachowski, B. and Gutkowski, W.: Effect of damaged circular flange-bolted connections on behaviour of tall towers, modelled by multilevel substructuring, Eng. Struct., Vol. 111, 93-103, 2016.

[19] Patil, C.S, Roy, S. and Jagtap, K.R.: Damage detection in frame structure using piezoelectric actuator, Mater. Today-Proc., Vol. 4, No. 2, Part A, pp. 687-692, 2017.

[20] Mori, K., Horibe, T. and Maejima, K.: Evaluation of the axial force in an FeCo bolt using the inverse magnetostrictive effect, Measurement, Vol. 165, Paper No. 108131, 2020.

[21] Yasui, H., Tanaka, H., Fujii, I. and Kawashima, K.: Ultrasonic measurement of axial stress in short bolts with consideration of nonlinear deformation, JSME Int. J. A-Solid M., Vol. 42, No. 1, pp. 111-118, 1999.

[22] Kim, N. and Hong, M.: Measurement of axial stress using mode-converted ultrasound, NDT&E Int., Vol. 42, No. 3, pp. 164-169, 2009.

[23] Blachowski, B., Swiercz, A., Gutkiewicz, P., Szelążek, J. and Gutkowski, W.: Structural damage detectability using modal and ultrasonic approaches, Measurement, Vol. 85, pp. 210-221, 2016.

[24] Pan, Q., Pan, R., Chang, M. and Xu, X.: A shape factor based ultrasonic measurement method for determination of bolt preload, NDT&E Int., Vol. 111, Paper No. 102210, 2020.

[25] Ren, L., Feng, T., Ho, M., Jiang, T. and Song, G.: A smart "shear sensing" bolt based on FBG sensors, Measurement, Vol. 122, pp. 240-246, 2018.

[26] Chen, D., Huo, L., Li, H. and Song G.: A fiber Bragg grating (FBG)-enabled smart washer for bolt pre-load measurement: design, analysis, calibration, and experimental validation, Sensors, Vol. 18, No. 8, Paper No. 2586, 2018.

[27] Wang, T., Chang, J., Gong, P., Shi, W., Li, N. and Cheng, S.: The experimental instrumented bolt with fibre Bragg grating force sensors, Arch. Min. Sci., Vol. 65, No. 1, pp. 179-194, 2020.

[28] Duan, C., Zhang, H., Li, Z., Tian, Y., Chai, Q., Yang, J., Yuan, L., Zhang, J., Xie, K. and Lv, Z.: FBG smart bolts and their application in power grids, IEEE T. Instrum. Meas., Vol. 69, No. 5, pp. 2515-2521, 2020.

[29] Martinez, J., Sisman, A., Onen, O., Velasquez, D. and Guldiken, R.: A synthetic phased array surface acoustic wave sensor for quantifying bolt tension, Sensors, Vol. 12, No. 9, pp. 12265-12278, 2012.

[30] Zhang, Z., Liu, M., Liao, Y., Su, Z. and Xiao, Y.: Contact acoustic nonlinearity (CAN)-based continuous monitoring of bolt loosening: Hybrid use of high-order harmonics and spectral sidebands, Mech. Syst. Signal Pr., Vol. 103, pp. 280-294, 2018.

[31] Wang, F., Ho, S.C.M. and Song, G.: Modeling and analysis of an impact-acoustic method for bolt looseness identification, Mech. Syst. Signal Pr., Vol. 133, Paper No. 106249, 2019.

[32] Wang, F., Ho, S.C.M., Huo, L. and Song G.: A novel fractal contact-electromechanical impedance model for quantitative monitoring of bolted joint looseness, IEEE Access, Vol. 6, pp. 40212-40220, 2018.

[33] Wang, C., Wang, N., Ho, S.-C., Chen, X., Pan, M. and Song G.: Design of a novel wearable sensor device for real-time bolted joints health monitoring, IEEE Internet Things, Vol. 5, No. 6, pp. 5307-5316, 2018.

[34] Huynh, T.-C., Nguyen, T.-D., Ho, D.-D., Dang, N.-L. and Kim, J.-T.: Sensor fault diagnosis for impedance monitoring using a piezoelectric-based smart interface technique, Sensors, Vol. 20, No. 2, Paper No. 510, 2020.

[35] Na, W.S.: Bolt loosening detection using impedance based non-destructive method and probabilistic neural network technique with minimal training data, Eng. Struct., Vol. 226, Paper No. 111228, 2021.

[36] Nazarko, P. and Ziemianski, L.: Force identification in bolts of flange connections for structural health monitoring and failure prevention, Procedia Structural Integrity, Vol. 5, pp. 460-467, 2017.

[37] Sun, J., Xie, Y. and Cheng, X.: A fast bolt-loosening detection method of running train's key components based on binocular vision, IEEE Access, Vol. 7, pp. 32227-32239, 2019.

[38] Wang, C., Wang, N., Ho, S.-C., Chen, X. and Song, G.: Design of a new vision-based method for the bolts looseness detection in flange connections, IEEE T. Ind. Electron., Vol. 67, No. 2, pp. 1366-1375, 2020.

[39] Huynh, T.-C.: Vision-based autonomous bolt-looseness detection method for splice connections: Design, lab-scale evaluation, and field application, Automat. Constr., Vol. 124, Paper No. 103591, 2021.

[40] Sidorov, M., Khor, J.H., Nhut, P.V., Matsumoto, Y. and Ohmura, R.: A public blockchain-enabled wireless LoRa sensor node for easy continuous unattended health monitoring of bolted joints: Implementation and evaluation, IEEE Sens. J., Vol. 20, No. 21, pp. 13057-13065, 2020.

[41] Ryś, J., Malara, P. and Barski, M.: Numerical analysis of the gasket stiffness influence on the bold load in flanged joints, Technical Transactions, Vol. 108, No. 5, pp. 93-112, 2011.

[42] Grudziński, P. and Konowalski, K.: Comparative studies of the seatings of propulsion plants and auxiliary machinery on chocks made of metal and cast of resin, Part 1: Mounting on steel chocks, Pol. Marit. Res., Vol. 26, No. 4, pp. 142-148, 2019.

[43] Pan, Q., Pan, R., Shao, C., Chang, M. and Xu, X.: Research review of principles and methods for ultrasonic measurement of axial stress in bolts, Chin. J. Mech. Eng., Vol. 33, Paper No. 11, 2020.

[44] Hosoya, N., Niikura, T., Hashimura, S., Kajiwara, I. and Giorgio-Serchi, F.: Axial force measurement of the bolt/nut assemblies based on the bending mode shape frequency of the protruding thread part using ultrasonic modal analysis, Measurement, Vol. 162, Paper No. 107914, 2020.

[45] Grzejda, R. and Parus, A.: Experimental studies of the process of tightening an asymmetric multi-bolted connection, IEEE Access, Vol. 9, pp. 47372-47379, 2021.

[46] Grzejda, R., Parus, A. and Kwiatkowski, K.: Experimental studies of an asymmetric multi-bolted connection under monotonic loads, Materials, Vol. 14, No. 9, Paper No. 2353, 2021.

[47] McCarthy, M.A., Lawlor, V.P., O'Donnell, P.C., Harris, K., Kelly, P. and Cunningham, J.P.: Measurement of bolt pre-load in torqued composite joints, Strain, Vol. 41, No. 3, pp. 109-112, 2005.

[48] Matos, R., Shah Mohammadi, M.R. and Rebelo, C.: A year-long monitoring of preloaded free-maintenance bolts – Estimation of preload loss on BobTail bolts, Renew. Energ., Vol. 116, Part B, pp. 123-135, 2018.

[49] Mekid, S., Bouhraoua, A. and Baroudi, U.: Battery-less wireless remote bolt tension monitoring system, Mech. Syst. Signal Pr., Vol. 128, pp. 572-587. 2019.

[50] Kawecki, P. and Kozlowski, A.: Experimental investigation of end-plate splices with multiple bolt rows of large girders, J. Constr. Steel Res., Vol. 167, Paper No. 105859, 2020.

[51] Hu, J., Zhang, K., Cheng, H. and Qi, Z.: An experimental investigation on interfacial behavior and preload response of composite bolted interference-fit joints under assembly and thermal conditions, Aerosp. Sci. Technol., Vol. 103, Paper No. 105917, 2020.

[52] Kiyokawa, S., Tateishi, K., Hanji, T. and Shimizu, M.: Slip coefficient and ultimate strength of high strength bolted friction joints with compact bolt spacing and edge distance, Int. J. Steel Struct., Vol. 19, No. 4, pp. 1191-1201, 2019.

[53] Li, Y., Liu, Z., Wang, Y., Cai, L. and Xu, W.: Research on preload of bolted joints tightening sequence-related relaxation considering elastic interaction between bolts, J. Constr. Steel Res., Vol. 160, pp. 45-53, 2019.

[54] You, R., Ren, L. and Song, G.: A novel comparative study of European, Chinese and American codes on bolt tightening sequence using smart bolts, Int. J. Steel Struct., Vol. 20, No. 3, pp. 910-918, 2020.

[55] Zhang, D., Zhou, J. and Mao, K.: Simulational and experimental study of stress in bolts work-piece, Journal of Measurements in Engineering, Vol. 8, No. 2, pp. 46-61, 2020.

[56] Kumakura, S. and Saito, K.: Tightening sequence for bolted flange joint assembly, in: *ASME 2003 Pressure Vessels and Piping Conference, Analysis of Bolted Joints*, 20-24.07.2003, Cleveland, Ohio, USA, pp. 9-16.

[57] Zhang, L.Z., Liu, Y., Sun, J.C., Ma, K., Cai, R.L. and Guan, K.S.: Research on the assembly pattern of MMC bolted flange joint, Procedia Engineering, Vol. 130, pp. 193-203, 2015.

[58] Zhu, L., Bouzid, A.-H., Hong, J.: Analytical evaluation of elastic interaction in bolted flange joints, Int. J. Pres. Ves. Pip., Vol. 165, pp. 176-184, 2018.

[59] Grzejda, R.: Impact of nonlinearity of the contact layer between elements joined in a multi-bolted system on its preload, International Journal of Applied Mechanics and Engineering, Vol. 22, No. 4, pp. 921-930, 2017.

[60] Grzejda, R.: Determination of bolt forces and normal contact pressure between elements in the system with many bolts for its assembly conditions, Adv. Sci. Technol. Res. J., Vol. 13, No. 1, pp. 116-121, 2019.

[61] PN-EN 1993-1-8, 2006. Eurocode 3: Design of Steel Structures, Part 1-8: Design of Joints, Polish Committee for Standardization, Warsaw, 2006.

ЛАБОРАТОРИЈСКА ПРОЦЕНА ВЕЗЕ СА ВИШЕ ВИЈАКА ЗБОГ УКЛАЊАЊА ИЗАБРАНИХ ВИЈАКА

Р. Грзејда, А. Парус

Приказано је експериментално истраживање асиметрично оптерећене везе са седам вијака.

Притезање везе је извршено кључем за вијке а праћење вредности сила обављено је калибрисаним уређајем за мерење напона. Испитиване су две методе притезања вијака: метод једног корака и метод више корака. После притезања свих вијака уклоњени су одабрани вијци, при чему је извршена симулација отказа вијака у условима оптерећења везе. Истражен је утицај методе и редоследа притезања вијака на дистрибуцију вредности вијачних сила и увођења стања отказа неких вијака. Резултати су статистички обрађени и графички приказани за све случајеве отказа са аспекта дистрибуције вредности нормализованих сила.